Table III. Values (kJ/mol) of $(\Delta G^\circ_{org} - \Delta G^\circ_{H_2O})_{solv}$[a] and $(\Delta G^\circ_{org} - \Delta G^\circ_{H_2O})_{lig}$ for Cu(Me$_6$[14]4,11-dieneN$_4$)$^{2+}$ Isomers with Various Anions at 25.0 ± 0.1 °C

X^-	$(\Delta G^\circ_{Me_2SO} - \Delta G^\circ_{H_2O})_{solv}$	$(\Delta G^\circ_{Me_2SO} - \Delta G^\circ_{H_2O})_{lig}$	
		N-rac-[CuL]$^{2+}$	*N-meso*-[CuL]$^{2+}$
Cl^-	46.0	−14.89	−14.88
Br^-	32.6	−11.79	−12.17
I^-	15.9	−7.88	−8.13
N_3^-	30.5	−11.76	−11.61
X^-	$(\Delta G^\circ_{DMF} - G^\circ_{H_2O})_{solv}$	$(\Delta G^\circ_{DMF} - \Delta G^\circ_{H_2O})_{lig}$	
		N-rac-[CuL]$^{2+}$	*N-meso*-[CuL]$^{2+}$
Cl^-	51.5	−18.78	−19.59
Br^-	40.2	−15.57	−16.26
I^-	23.4	−10.52	−11.26
N_3^-	38.5	−14.73	−15.34
X^-	$(\Delta G^\circ_{MeOH} - \Delta G^\circ_{H_2O})_{solv}$	$(\Delta G^\circ_{MeOH} - \Delta G^\circ_{H_2O})_{lig}$	
		N-rac-[CuL]$^{2+}$	*N-meso*-[CuL]$^{2+}$
Cl^-	14.2	−22.07	−22.93
Br^-	12.1	−19.37	−19.24
I^-	8.4	−12.72	−12.77
N_3^-	10.5	−17.69	−17.81

[a] See ref 11.

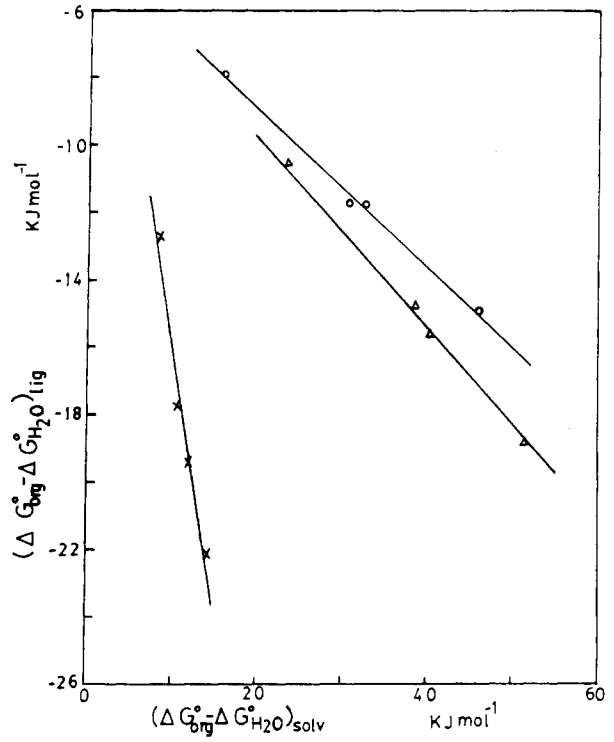

Figure 4. Plot of $(\Delta G^\circ_{H_2O})_{lig}$ against $(\Delta G^\circ_{org} - \Delta G^\circ_{H_2O})_{solv}$ at 25.0 ± 0.1 °C for Cu(*N-rac*-Me$_6$[14]4,11-dieneN$_4$)$^{2+}$: △, DMF; ○, Me$_2$SO; ×, MeOH.

on the extent of solvation of the monodentate ligands and the complexation in this study is mainly electrostatic.

Acknowledgment. The support of the Chemistry Research Center, National Science Council of the Republic of China, under Grants NSC 74-0208-M007-08 and NSC 75-0208-M007-04 is gratefully acknowledged.

Registry No. [Cu(*N-rac*-1,7-CT)]$^{2+}$, 48186-23-8; [Cu(*N-meso*-1,7-CT)]$^{2+}$, 48186-22-7; Cl^-, 16887-00-6; Br^-, 24959-67-9; I^-, 20461-54-5; N_3^-, 14343-69-2; DMF, 68-12-2; Me$_2$SO, 67-68-5; MeOH, 67-56-1.

Supplementary Material Available: Tables A–C, showing the values of apparent molar absorptivities for Cu(*N-rac*-Me$_6$[14]4,11-dieneN$_4$)$^{2+}$–X$^-$ and Cu(*N-meso*-Me$_6$[14]4,11-dieneN$_4$)$^{2+}$–X$^-$ systems as a function of [X$^-$] in DMF, Me$_2$SO, and MeOH, respectively, and Figures A and B, plots of ln K_X vs. ln $(1/D)$ and $(\Delta G^\circ_{org} - \Delta G^\circ_{H_2O})_{lig}$ vs. $(\Delta G^\circ_{org} - \Delta G^\circ_{H_2O})_{solv}$ (5 pages). Ordering information is given on any current masthead page.

Contribution from the Radiation Laboratory, University of Notre Dame, Notre Dame, Indiana 46556

Sequential Biphotonic Processes: Photochemical Reactivity of Phthalocyanine Radicals

B. Van Vlierberge and G. Ferraudi*

Received July 22, 1986

Phthalocyanine radicals have been generated by chemical and photochemical means, and it is possible to consider them as common intermediates in redox reactions of metallophthalocyanines.[1,2] From a structural standpoint, these species, related to porphyrin radicals, are very likely species with an unpaired electron in a ligand-centered molecular orbital.[3] Previous work on the photochemistry of Rh(III) phthalocyanine cation radicals has shown that these species undergo different photochemical transformations for excitations in the UV and vis bands, respectively.[1] The UV excitation results in the reduction of the radical and oxidation of the solvent, a photoprocess associated with the abstraction of hydrogen from the solvent by $n\pi^*$ ligand-centered excited states. Moreover, photodecomposition of the radical is induced by irradiation at wavelengths longer than 500 nm. Such UV and vis photoreactivities can be related to the population of different photoreactive states, i.e. $\pi\pi^*$, $n\pi^*$ ligand-centered states and charge-transfer states. Insofar as the position of the charge-transfer states (relative to ligand-centered states) depends on the metal center, the photochemical properties exhibited by a series of phthalocyanine radicals differing in the metal center can be used as a probe of the charge-transfer-state participation in the photodecomposition of the radicals. In this regard, the photochemistries of Rh(III), Al(III), and Zn(II) phthalocyanine cation radicals have been investigated in this work.

Experimental Section

Photochemical Procedures. A flash photolysis apparatus, based on the synchronous triggering of two flash-lamp-pumped dye lasers, was used for the time resolution of optical events in sequential biphotonic photolyses (Figure 1). For these experiments we used a side-on excitation, i.e. with the monitoring light beam crossing the laser beams at a right angle. The overlap of the beams was regularly verified by either burning Polaroid film or maximizing the concentration of excited state produced by the excitation of various metallophthalocyanines. A fraction of the laser light was aimed at photodiodes in order to obtain reports concerning the intensity of the pulses and their relative delay. The time-resolved change in optical density induced by the sequential excitation was obtained as an average of 5–10 experiments, whereas the 100 data points of each experiment were obtained by subtracting two traces, corresponding each of them to the excitation of the photolyte with one of the two lasers from the trace recorded in the sequential excitation with both lasers. In this manner, the time-resolved net change in optical density corresponds to processes induced by the biphotonic irradiation. Namely, any contribution from monophotonic irradiations (λ_1 or λ_2 in Figure 1) has been removed from the one induced by the sequential irradiation ($\lambda_1 + \lambda_2$ in Figure 1). Other experimental conditions used in connection with the sequential biphotonic excitation of phthalocyanines have been described elsewhere.[4-6]

Materials. Literature reports were followed for the preparation and purification of $[Co(bpy)_3](ClO_4)_3$ (bpy = bipyridine).[7] The pure Rh(III) phthalocyanines were available from a previous work.[5,6] Eastman chloro(phthalocyaninato)aluminum(III), Al(pc)Cl, and zinc phthalocyanine, Zn(pc), were recrystallized three times from suitable solvents. Other materials were reagent grade and used without further purification.

(1) Ferraudi, G.; Oishi, S.; Muralidharan, S. *J. Phys. Chem.* **1984**, *88*, 5261 and references therein.
(2) Ferraudi, G.; Geiger, D. K.; Madden, K.; Granifo, J.; Rillema, D. P. *J. Phys. Chem.* **1985**, *89*, 3890.
(3) Barley, M.; Becker, J. Y.; Domazetis, G.; Dolphin, D.; James, B. R. *J. Chem. Soc., Chem. Commun.* **1981**, 982.
(4) Muralidharan, S.; Ferraudi, G. *J. Phys. Chem.* **1983**, *87*, 4877.
(5) Ferraudi, G. *J. Phys. Chem.* **1984**, *88*, 3938.
(6) Muralidharan, S.; Ferraudi, G.; Schmatz, K. *Inorg. Chem.* **1982**, *21*, 2961.
(7) Maki, N. *Bull. Chem. Soc. Jpn.* **1969**, *42*, 2275.

0020-1669/87/1326-0337$01.50/0

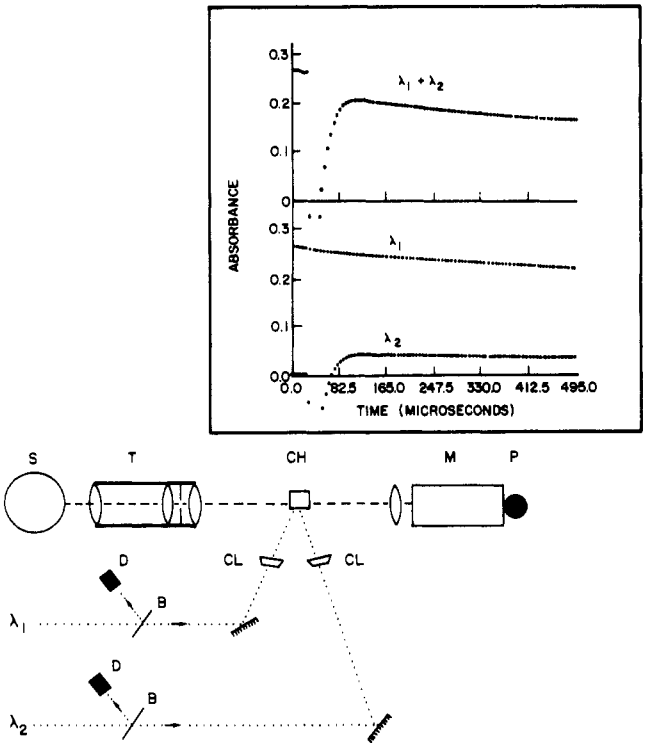

Figure 1. Optical arrangement used for sequential biphotonic irradiations in flash photolysis experiments: S, monitoring source; T, telescope; CH, cell holder; M, monochromator; P, phototube; CL, cylindrical lens; B, beam splitter, D, photodiode. The insert shows traces collected when samples of Zn(pc) in Me_2SO were irradiated with both lasers ($\lambda_1 + \lambda_2$) and with each of the lasers (λ_1 and λ_2). In a given experiment, the normalized traces obtained by irradiating with each laser will be subtracted from the trace obtained in sequential irradiations with both lasers.

Results

Photogeneration and Photoreactivity of Phthalocyanine Radicals. The excitation of the metallophthalocyanines at wavelengths of the phthalocyanine's Q band, $\lambda \approx 640$ nm, produced the long-lived triplet state (eq 1). The phthalocyanine radical was generated

$$M(pc) \rightleftharpoons (^3E)M(pc) \quad (1)$$

by quenching this excited state with $Co(bpy)_3^{3+}$ (eq 2). Lifetimes

$$(^3E)M(pc) + Co(bpy)_3^{3+} \rightarrow M(pc)^+ + Co(bpy)_3^{2+} \quad (2)$$

of the excited metallophthalocyanines and rates of quenching have been found to be in good agreement with literature reports,[8-10] while observations in a millisecond time domain show the regeneration of the phthalocyanines by back-electron-transfer reactions of the Co(II) complex with phthalocyanine radicals (eq 3). Moreover, irradiation of the phthalocyanine radicals with

$$M(pc)^+ + Co(bpy)_3^{2+} \rightarrow M(pc) + Co(bpy)_3^{3+} \quad (3)$$

a second laser pulse, $\lambda_{exc} \approx 520$ nm, results in a bleach of the optical density at wavelengths of the radical absorption maxima, $\lambda_{max} \approx 510$–$520$ nm, within the time resolution of our apparatus (Figure 1). The bleached absorbance is partially restored at longer times with a rate that depends on the concentration of photolyzed radical, i.e. on the optical density (ΔOD_p) bleached by the 520-nm laser pulse. The analysis of the reaction kinetics (Figure 2 and Appendix) gives first- and second-order dependences of the rate of recovery on the concentration of photolyzed radical at low and high concentrations of bleached radical, respectively.

Quantum Yields. Low concentrations of phthalocyanine radicals were used for the determination of quantum yields, $\phi = \Delta[M(pc)^+]/n_{h\nu}$, where $\Delta[M(pc)^+]$ represents the concentration of photolyzed radical and $n_{h\nu}$ the photonic concentration absorbed (per pulse). This photonic concentration is related to the concentration of radical generated by the synthesizing pulse by eq 4, where $n_{h\nu}^0$ is the incident photonic concentration, l_y is the

$$n_{h\nu} = n_{h\nu}^0(1 - \exp[2.303 l_y \epsilon [M(pc)^+]]) \approx 2.303 n_{h\nu}^0 l_y \epsilon [M(pc)^+] \quad (4)$$

transverse optical path, and $[M(pc)^+]$ is the radical concentration at the arrival of the photolyzing pulse. Moreover, the concentration of radical, $[M(pc)^+]$, and the concentration of photolyzed radical, $\Delta[M(pc)^+]$, can be estimated from the corresponding changes of the optical density caused by the synthesizing pulse ΔOD_s and the photolyzing pulse $\Delta OD_p(0)$. Introduction of eq 4 into the definition of the quantum yields given above leads to

$$\phi \approx \frac{1}{2.303 l_y \epsilon n_{h\nu}^0} \frac{\Delta OD_p(0)}{\Delta OD_s} \quad (5)$$

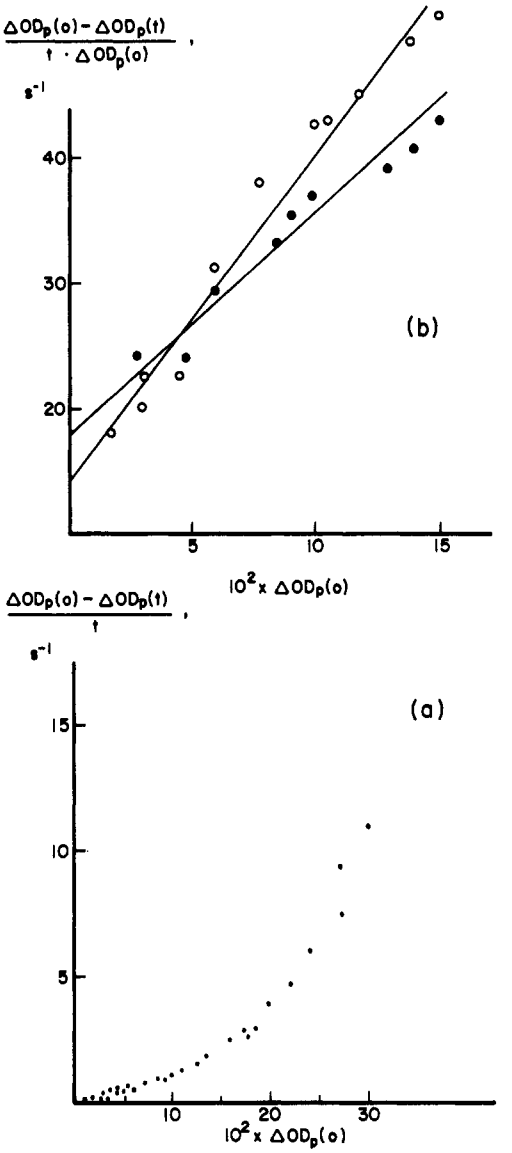

Figure 2. Typical plots for the study of the transient kinetics (Appendix) as a function of the amount of photolyzed radical. In the ordinate, $\Delta OD_p(0)$ and $\Delta OD_p(t)$ represent the change in optical density induced by the photolyzing pulse at two different instants, 0 and t, of the reaction. The deviation from linearity in (a) signals departures from a first-order kinetics while linearized plots (b) give information about the rate constants for the first-order (intersect) and the second-order (slope) kinetics. The results of 520-nm photolyses in (a) were determined with $Zn(pc)^+$ and in (b) with $Al(pc)Cl^+$ (○) or $Rh(pc)Br^+$ (●) in deaerated Me_2SO.

(8) Ohno, T.; Kato, S. *J. Phys. Chem.* **1984**, *88*, 1670.
(9) Muralidharan, S.; Ferraudi, G. *Inorg. Chem.* **1981**, *20*, 462.
(10) Frink, M. E.; Geiger, D. K.; Ferraudi, G. *J. Phys. Chem.* **1986**, *90*, 1924.

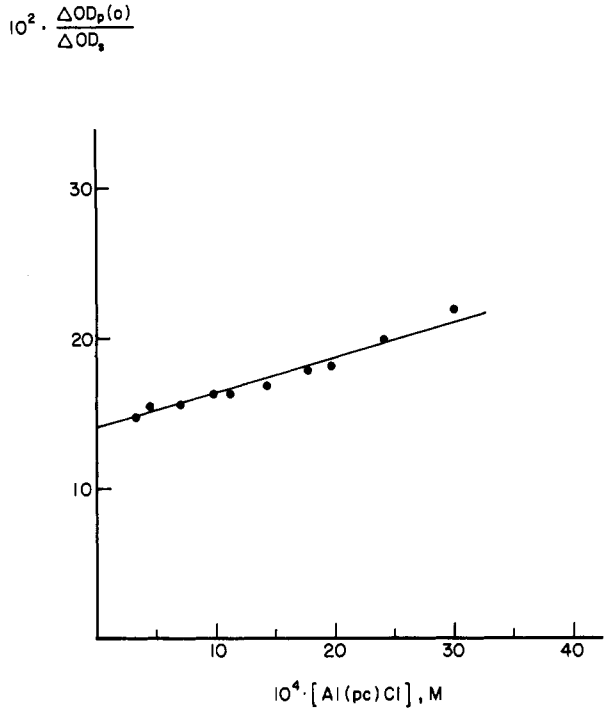

Figure 3. Dependence of $\Delta OD_p(0)/\Delta OD_s$ on the concentration of radical, e.g. ΔOD_s, produced by the synthesizing pulse. The results in the figure were determined with Al(pċ)Cl$^+$ in Me_2SO by varying either or both the concentration of Al(pc)Cl and the intensity of the 520-nm photolyzing pulse.

Table I. Quantum Yields for the Decomposition of Phthalocyanine Radicals

radical	$10^2\phi$[a]	medium[b]
Rh(pċ)Br$^+$	2.8	Me_2SO
	1.3	30% H_2O in Me_2SO
	2.3	30% H_2O in 2-propanol
Rh(pċ)Cl$^+$	1.3	30% H_2O in 2-propanol
Al(pċ)Cl$^+$	1.9	Me_2SO
	0.8	30% H_2O in Me_2SO
	1.7	30% D_2O in Me_2SO
	0.4	30% H_2O in 2-propanol
Zn(pċ)$^+$	2.7	Me_2SO
	1.2	15% H_2O in Me_2SO

[a] Experimental errors less than 5%. [b] Solutions deaerated with streams of ultrapure N_2.

Insofar as the validity of eq 5 is limited to optically diluted solutions, quantum yields were determined by extrapolation to a zero phthalocyanine concentration (Figure 3). Quantum yields for the photodecomposition of the phthalocyanine radicals are reported in Table I. The yields do not depend on the metal center but exhibit a marked dependence on the medium. Such a medium dependence is also observed for the replacement of water by perdeuteriated water.

Discussion

The 520-nm irradiation of the phthalocyanine radicals leads to a rapid, i.e. $t < 1$ μs, decomposition of these species, followed by a partial recovery of the radical concentration. Such a recovery exhibits a complex kinetics, which has been interpreted as involving competitive processes with first- and second-order dependences, respectively, on the concentration of photolyzed radical, i.e. the equivalent concentration of the reaction intermediate I (eq 6–9).

$$M(pċ)^+ \overset{h\nu}{\rightleftharpoons} {}^*M(pċ)^+ \rightarrow I \quad (6)$$

$$I \rightarrow M(pċ)^+ \quad (7)$$

$$I \rightarrow \text{decomposition products} \quad (8)$$

$$I + I \rightarrow M(pċ)^+ + \text{decomposition products} \quad (9)$$

Table II. Rate Constants for Decomposition/Regeneration of Phthalocyanine Radicals

radical[a]	$10^{-1}k_7$, s^{-1}	$10^{-1}k_8$, s^{-1}	$10^{-6}k_9$,[b] $M^{-1}\ s^{-1}$
Rh(pċ)Br$^+$	1.4	7.1	5.2
Al(pċ)Cl$^+$	1.8	9.0	4.6
Zn(pċ)$^+$	1.3	2.5	4.1

[a] Determination in deaerated Me_2SO. [b] Values calculated with the following absorption coefficients: 1.8×10^4 (510 nm) for Rh(pċ)Br$^+$; 2.9×10^4 (520 nm) for Al(pċ)Cl$^+$; 2.9×10^4 (510 nm) for Zn(pċ)$^+$.

Following an earlier report on the photodecomposition of Rh(III) phthalocyanine radicals,[1] fragments of the ring opening in eq 8 and 9 are described as decomposition products. Moreover, the partial recovery of phthalocyanine radical observed in flash photolysis suggests that the macrocycle is still closed in the species I, while the lack of intense optical absorptions over the 450–600-nm region could be seen as a consequence of disruption in the delocalization of the macrocycle's π system. In these contexts, it is possible to describe the intermediate I as an isomer of the M(pċ)$^+$ radical with a nonplanar macrocycle that can either decompose (eq 8 and 9) or regenerate the ligand in the parent radical (eq 7 and 9). In this mechanism, the observed time evolution of the radical concentration, i.e. the recovery, is a consequence of the slow reactions 7–9, while the process leading to the formation of the intermediate I, eq 6, is too fast for the apparatus time resolution. The values of the rate constants for those processes with a first-order dependence on the concentration of photodecomposed phthalocyanine radical, i.e. radical regeneration, k_7, and intermediate I decomposition, k_8, signal that the intermediates produced from Rh(III) and Al(III) radicals have nearly the same reactivity and that this is larger than the reactivity exhibited by the Zn(II) species (Table II). Moreover, the regeneration of the parent radical via a second-order process (eq 9) suggests that association of the intermediate I might facilitate a structural reorganization leading to the products' formation. It is possible that such a metal-dependent reactivity reflects, in either or both the first- and second-order rates, the effect of the metal charge over the macrocycle, i.e. in a manner that resembles the dependence of the phthalocyanine redox potential on the ionic potential of the metal center.

The quantum yields reported in Table I can be regarded as a measure of the excited-state ability to produce I through competitive reactions (eq 6), a photoreactivity that, for Rh(III) radicals, has been proposed to be associated with the population of charge-transfer excited states. Such low-energy charge-transfer states are not expected to be available for the Al(III) and Zn(II) radicals, and their photoreactivities must be related, therefore, to $n\pi^*$ and/or $\pi\pi^*$ ligand-centered states. Insofar as Rh(III), Al(III), and Zn(II) radicals exhibit similar photoreactivities, the significance of the charge-transfer excited states dims in the photochemistry of Rh(III) radicals. In this regard, the dependence of the yield on medium conditions is likely related to an increase in the yield of the reactive excited state and/or a decrease in the rate of excited-state relaxation (eq 6) in changing from protic to aprotic media or replacing D_2O by H_2O, effects that are expected when the excited molecules can be associated to the solvent by hydrogen bonding.

Acknowledgment. The research described herein was supported by the Office of Basic Energy Sciences of the Department of Energy. This is Document No. NDRL-2885 from the Notre Dame Radiation Laboratory.

Appendix

The rate constants (Table II) for eq 6–9 were calculated by resolving the rate equation

$$-d[I]/dt = (k_7 + k_8)[I] + 2k_9[I]^2$$

for the decay of the intermediate I with a series

$$[I] = [I]_0 \sum_{i=0}^{\infty} a_i t^i$$

The initial condition, $[I] = [I]_0$ at $t = 0$, leads to the coefficients

$$a_0 = 1$$

$$a_1 = -(k_7 + k_8 + 2k_9[I]_0)$$

$$a_2 = \tfrac{1}{2}a_1^2 \ldots$$

$$a_3 = \tfrac{1}{6}a_1^3 \ldots$$

Series describing the time dependences of the radical concentration and optical density were obtained by a similar treatment.[11] The corresponding series for the change in the optical density, ΔOD, is

$$\Delta OD_p(t) = [\Delta OD_p(0)]\left[1 - \left(k_7 - \frac{k_9[\Delta OD_p(0)]}{\epsilon l}\right)t - \left(\frac{k_7}{2} - \frac{k_9[\Delta OD_p(0)]}{\epsilon l}\right)a_1 t^2 - \ldots\right]$$

This expression was recast in the form

$$\frac{\Delta OD_p(0) - \Delta OD_p(t)}{t[\Delta OD_p(0)]} \approx k_7 - \frac{k_9}{\epsilon l}\Delta OD_p(0)$$

for the graphic representation of the experimental data (Figure 2). Moreover, the values of k_7 and k_9 together with values for the initial and final ΔOD_p, e.g. $\Delta OD(0)$ and $\Delta OD(\infty)$, were used for the calculation of k_8.

Registry No. pc, 574-93-6; Rh(pc)Br$^+$, 105900-44-5; Rh(pc)Cl$^+$, 105900-45-6; Al(pc)Cl$^+$, 57650-26-7; Zn(pc)$^+$, 53029-44-0.

(11) The extinction coefficient of the intermediate I has been regarded to be insignificant in relationship to the extinction coefficient of M(pc)$^+$, a proposition that is in agreement with the structure proposed for I.

Contribution from the Laboratoire de Cinétique Chimique and Laboratoire de Chimie des Métaux de Transition, Université Pierre et Marie Curie, 75230 Paris Cedex 05, France

Synthesis and Structure of $[W_2(S)_2(\mu\text{-}S)(\eta^2\text{-}S_2)_4]^{2-}$, a Novel Binary Sulfide Derived from the Acidification of WS_4^{2-}

J. M. Manoli,*† C. Potvin,† and F. Sécheresse‡

Received June 25, 1986

$[M'(MS_4)_2]^{2-}$ complexes (with M = Mo, W and M' = Zn, Ni, Fe, Co, Pd, Pt)[1] have been synthesized, and structural determinations by X-ray diffraction have been reported for these complexes. In an attempt to prepare the $[Mn(MS_4)_2]^{2-}$ dianion, we have isolated with M = W a dark red crystalline material that was identified by elemental analysis as an unexpected new tungsten sulfide.

The synthesis of the molybdenum analogue was not successful; instead, we isolated the anion $Mo_3S_9^{2-}$.[2] Here we report the synthesis, isolation, and structural characterization of a new binary W-S complex.

Experimental Section

All manipulations were carried out in air; chemicals were used as purchased.

$(PPh_4)_2W_2S_{11}$. A solution of 0.375 g (0.38 mmol) of $(PPh_4)_2WS_4$ in 32 mL of CH_3CN was acidified with 0.15 mL of glacial acetic acid. After addition of a solution of 0.15 g (0.75 mmol) of $MnCl_2 \cdot 4H_2O$[3] in 2 mL of CH_3OH the mixture turned immediately deep red. The resulting solution was stirred for 1 h, allowed to stand ca. 1 h at room temperature, and then filtered and cooled in a closed flask under argon to -10 °C. After 24 h analytically pure, well-shaped, large dark red crystals were obtained (70 mg), which were separated from the filtrate, washed with small amounts of ether, and air-dried. Anal. Calcd for $C_{50}H_{43}NP_2W_2S_{11}$: C, 41.7; S, 24.5; P, 4.3; W, 25.5. Found: C, 40.8; S, 25.9; P, 4.3; W, 25.1.

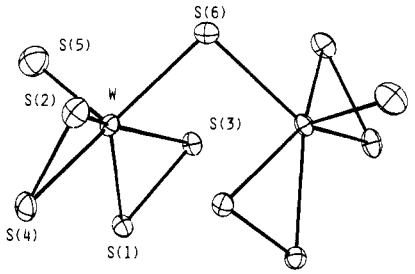

Figure 1. Perspective view (50% ellipsoids) of the $W_2S_{11}^{2-}$ anion showing the atom-labeling scheme. Half of the anion is generated through a binary axis passing through the S(6) atom.

$(PPh_4)_2Mo_3S_9$. This complex was prepared in a manner similar to that for the previous one. Within 1-3 days at -10 °C, dark red needlelike crystals were obtained. The IR spectra and the X-ray space group of the compound were identical with those of $(PPh_4)_2Mo_3S_9$.[2]

Physical Measurements. Electronic spectra were recorded at 20 °C on a Kontron 810 spectrophotometer between 600 and 200 nm. Solutions of the compound in CH_3CN were about 1 mg mL^{-1}. Infrared spectra (KBr pellet) were recorded on a Perkin-Elmer 580B spectrophotometer.

Crystal Structure Determination. The unit cell dimensions and space group were determined from preliminary oscillations and Weissenberg photographs. The symmetry was monoclinic, and the systematic absences led to the $C2/c$ or Cc space group. A single crystal of dimensions 0.12 × 0.17 × 0.34 mm was selected and mounted on a Nonius CAD 4 automatic diffractometer equipped with Mo Kα radiation and a graphite monochromator. Least-squares calculations on 25 high-angle reflections collected at 20 °C yielded a monoclinic cell of dimensions a = 20.724 (6) Å, b = 20.367 (3) Å, c = 12.452 (3) Å, β = 99.52 (2)°, and V = 5183 Å^3.

Other details of data collection were as follows: scan mode $\theta/2\theta$, scan rate variable, scan range calculated by 1.00 + 0.34 tan θ with 25% extension on each side for backgrounds. Three orientation standards were checked every 100 observations. Three intensity monitors were checked every hour and remained constant. The calculated density was 1.85 g cm^{-3} with Z = 4 formula units per cell. A total of 5284 reflections ($\pm h, +k, +l$) were measured up to θ_{max} = 25°; after averaging 4207 were obtained, and among them, 3224 with $F_o > 4\sigma(F_o)$ were the final data set. Lorentz and polarization corrections were applied to the data. No absorption correction was made.

The centrosymmetric space group $C2/c$ was first assumed and gave satisfactory refinement. The structure was solved by the heavy-atom method. A three-dimensional Patterson map revealed the position of the tungsten atom. Successive refinements and difference Fourier maps revealed the locations of the remaining atoms (S, P, and C of the phenyl rings). The refinement with isotropic thermal parameters for all located atoms gave a R value of 0.098 for 2957 observations. At this stage a difference Fourier exhibited peaks that were attributed to a solvent molecule (CH_3CN). Riding isotropic hydrogen atoms were included in the refinement subject to the constraints C-H = 1.08 Å and U(H) = 1.1[U(C)], where U(C) is the equivalent isotropic thermal parameter of a carbon atom of the phenyl ring. Additional cycles of refinement with anisotropic temperature factors for W, P, and S and isotropic thermal parameters for all other atoms converged to conventional values of R = 0.0402 and R_w = 0.036 with a GOF of 0.67. All computations were performed by using SHELX76 on a Gould Concept 32/87 computer. Neutral atomic scattering factors and correction for anomalous dispersion were obtained from ref 4. Final atomic positional parameters were found

† Laboratoire de Cinétique Chimique.
‡ Laboratoire de Chimie des Métaux de Transition.

(1) (a) Müller, A.; Diemann, E.; Jostes, R.; Bögge, H. *Angew. Chem., Int. Ed. Engl.* **1981**, *20*, 934 and references therein. (b) Callahan, K. P.; Piliero, P. A. *Inorg. Chem.* **1980**, *19*, 2609.
(2) Pan, W. H.; Leonowicz, M. E.; Stiefel, E. I. *Inorg. Chem.* **1983**, *22*, 672.
(3) At the suggestion of a reviewer we have shown from complementary experiments that a methanolic solution of LiCl leads to the formation of only $W_3S_9^{2-}$. Furthermore, a solution of $CrCl_3$ produces only $W_4S_{12}^{2-}$. These results are consistent with the need for $MnCl_2$ to synthesize $W_2S_{11}^{2-}$.
(4) Cromer, C. T.; Waber, J. T. *International Tables for X-ray Crystallography*; Kynoch: Birmingham, England, 1974; Vol. IV, Tables 2.2.A and 2.3.1.

0020-1669/87/1326-0340$01.50/0